NANO LETTERS

2008
Vol. 8, No. 5
1456-1460

Three-Dimensionally-Patterned Submicrometer-Scale Hydrogel/Air Networks That Offer a New Platform for Biomedical Applications

Ji-Hyun Jang,[†] Shalin J. Jhaveri,[‡,§] Boris Rasin,[†] ChoengYang Koh,[†] Christopher K. Ober,[*,‡] and Edwin L. Thomas[*,†]

Institute for Soldier Nanotechnologies, Department of Materials Science and Engineering, Massachusetts Institute of Technology, Cambridge, Massachusetts 02139, and Department of Materials Science and Engineering and Department of Chemistry and Chemical Biology, Cornell University, Ithaca, New York, 14853

Received February 14, 2008; Revised Manuscript Received March 8, 2008

ABSTRACT

Phase mask interference lithography was employed to fabricate three-dimensional (3D) hydrogel structures with high surface area on neural prosthetic devices. A random terpolymer of poly(hydroxyethyl methacrylate-*ran*-methyl methacrylate-*ran*-methacrylic acid) was synthesized and used as a negative-tone photoresist to generate bicontinuous 3D hydrogel structures at the submicrometer scale. We demonstrated that the fully open 3D hydrogel/air networks can be used as a pH-responsive polymeric drug-release system for the delivery of neurotrophins to enhance the performance of neural prosthetic devices. Additionally an open hydrogel structure will provide direct access of neuronal growth to the device for improved electrical coupling.

Interfacing the nervous system with electronic devices for recording and/or stimulation purposes holds great promise for acquiring a new understanding of nervous system function as well as for treatment following injury or disease. Human control of robotic movements is also possible using recording devices for the brain−computer interface.[1,2] In general, deep brain stimulators are being employed for treating Parkinson's disease[3] and movement disorders while cochlear implants are being used to treat hearing loss.[4] Using the methods for silicon processing borrowed from the microelectronics industry, researchers have begun to microfabricate neural prosthetic devices for stimulation and chronic recording of nerve cells.[5,6] These miniature devices can cause considerably less tissue damage and more focused stimulation than larger versions.[7] However, there are considerable challenges before these devices can be fully exploited. One of the main drawbacks is a decrease in performance of the device over a period of days to weeks. This is caused by reactive cellular responses resulting in glial scar formation.[8,9] The scar tissue formation has been hypothesized to be caused by short-term and long-term responses. The short-term responses are due to damage associated with device insertion,[7,10] while long-term, sustained responses result from brain−device interactions.[11] To address this problem, researchers have either selected more biocompatible materials, modified the surfaces of devices to control cell attachment and interaction, or used local drug-delivery systems for release of anti-inflammatory agents.[12–14] Although these approaches are essential steps towards the improvement of existing devices, a real practical solution to counter this problem has not yet been reported.

Patterned hydrogel structures have been widely used for applications in biosensors, diagnostic assay systems, and microlens arrays due to their biocompatibilities and physically tunable properties.[15–18] The use of sophisticated three-dimensional (3D) hydrogel structures would enable important advances in drug delivery, tissue engineering, and favorable material−device interaction.[19–23] For example, 2D cell cultures do not properly imitate the microambiance of three-dimensionally-organized native tissue. Techniques for the synthesis of 3D structures can be broadly classified into bottom-up and top-down approaches, each with its own advantages and disadvantages. Bottom-up approaches based on the self-assembly of block copolymers or colloids are cheaper and can cover relatively large areas but have problems with defects and limitations in the range of structures that can be formed. So far most 3D hydrogel

* Corresponding authors: Edwin L. Thomas, tel (617) 253-6901, fax (617) 253-5859, e-mail elt@mit.edu; Christopher K. Ober, tel (607) 255-8417, fax (607) 255-2365, e-mail cober@ccmr.cornell.edu.

† Institute for Soldier Nanotechnologies, Department of Materials Science and Engineering, Massachusetts Institute of Technology.

‡ Department of Materials Science and Engineering, Cornell University.

§ Department of Chemistry and Chemical Biology, Cornell University.

10.1021/nl080444+ CCC: $40.75
Published on Web 04/05/2008

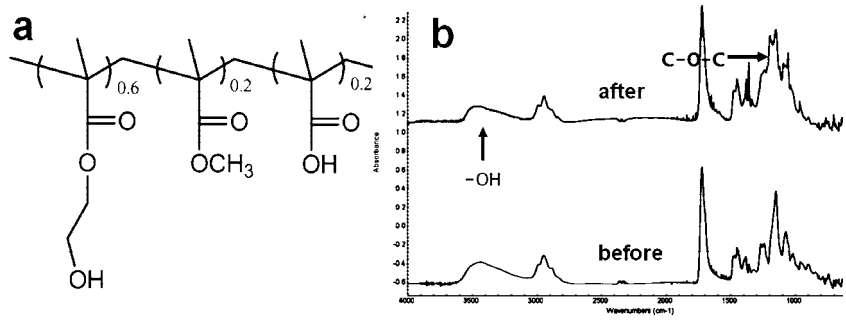

Figure 1. (a) Schematic diagram of the poly(HEMA-MMA-MAA) random terpolymer. (b) FT-IR spectrum of poly(HEMA-MMA-MAA) as spun and after exposure and postexposure bake (PEB).

structures have been made by infiltration into colloidal crystal scaffolds that are self-assembled by thermodynamic forces, followed by UV curing of their precursors and finally removal of the template by solvent.[24,25] As a result, the inverted hydrogel structures have additional defects arising from the second transfer process as well as the limitations present in the original template. The ability to fabricate 3D hydrogels (microgels) with controlled geometry and feature sizes is important since pore size and shape strongly impact cell behavior in many biomedical applications such as tissue engineering and biosensors.[26,27] Top-down approaches such as layer by layer assembly, dip-pen lithography, and two-photon lithography are some of the techniques that have been used for microfabrication of arbitrary structures, but these are rather time-consuming processes.[28] Phase mask interference lithography (PMIL) uses an elastomeric phase mask to make complex 3D structures. By flood exposing a thick spin-coated photoresist with a collimated beam through a suitably designed phase mask, one can make complex 3D structures over a large area. While the technique is still in an early phase of development, the method has been successfully employed by the Rogers group[29] and Thomas group[30] to fabricate complex 3D periodic and quasi-periodic structures at the submicrometer scale. So far, however, PMIL has been typically performed using commercially available photoresist materials such as SU-8, which is unsuitable for tissue engineering, biosensors, or drug-delivery applications where biocompatibility, functionalization, and drug loading of the materials is essential.

Recently, 3D hydrogel structures from liquid oligomer were fabricated in a microfluidic device with an integrated phase mask via stop-flow interference lithography.[31] However, low contrast of the particular photoresists arising from the uncontrollable rate of radical polymerization induces relatively high cross-linking density in the unexposed region resulting in not fully open 3D hydrogels even at the micrometer scale. It is necessary to be able to both generate open bicontinuous 3D hydrogel structures over large areas and produce tailor-made materials for specific applications with prescribed geometry and much finer feature sizes. Here, we report the use of PMIL to 3D pattern a newly designed biocompatible polymer, resulting in a hydrogel, which has fully open (i.e., bicontinuous polymer/air) and submicrometer scale structures. We show that the entire area of a neural prosthetic device can be coated with such 3D hydrogel/air networks. Additionally, our hydrogel system is shown to be able to release neurotrophins in a controlled manner over a short period of time. Thus, this multifunctional coating addresses all of the shortcomings cited previously.

A schematic diagram of the photoresist we employ is shown in Figure 1a. Our photoresist is composed of three monomers: 2-hydroxyethyl methacrylate (HEMA), methyl methacrylate (MMA), and methacrylic acid (MAA). A random terpolymer of poly(HEMA-*r*-MMA-*r*-MAA) was synthesized via radical polymerization (see Supporting Information) and used as a negative-tone photoresist to create bicontinuous 3D hydrogel structures. We aimed to design the polymer such that it cross-links via chemical amplification processes employing cationic polymerization. This approach is superior to radical polymerization, in which the fast diffusion of radicals and the accompanied refractive index change during polymerization result in less control over microstructure formation.[32,33] Poly(HEMA) is a widely used hydrogel that swells in aqueous solution and has been used in many biomedical applications, such as tissue implant, drug delivery, and contact-lens applications.[34] In this negative-tone resist system, the structure can be written by light-induced cross-linking of the hydroxyl groups of poly(HEMA) via a cross-linker (TMMGU, tetramethoxymethyl glycoluril) which in turn is activated by a photoacid generator.[35] FT-IR spectra before and after exposure and postexposure bake are shown in Figure 1b. The peak intensity around 3600–3000 cm^{-1} due to the hydroxyl group decreases, whereas the peak intensity around 1180 cm^{-1} due to the formation of C−O−C linkages after PEB increases, verifying that the expected cross-linking reaction between hydroxyl groups and the cross-linker has occurred. Therefore, the solubility change of the resist film in the exposed region is attributed to the acid-catalyzed cross-linking reaction and formation of less polar C−O−C linkages. Poly(MMA) and poly(MAA) have also been used for many biological applications.[36,37] MAA is incorporated in order to make the polymer responsive to various pH conditions which can be used to make a smart drug-delivery system. MMA is added to the polymer as a modifier which facilitates lithography through higher solubility in common solvents and increased T_g of the formed structures, resulting in more robust structures.

The 3D bicontinuous polymer/air structures are fabricated via laser-initiated cationic polymerization. The transfer of the interference pattern from the set of exit beams of light

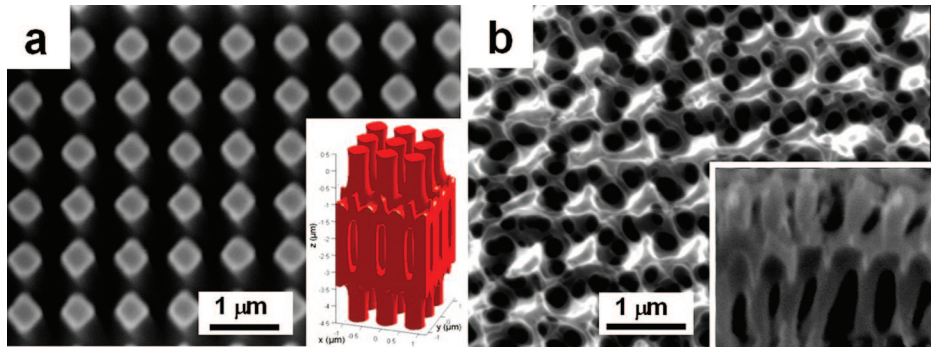

Figure 2. Comparison between theoretical and experimental structures: (a) The SEM image of the PDMS phase mask with a 2D periodicity of 760 nm. The posts of the phase mask in (a) have a height of 350 nm and spacing of 760 nm. The inset is the perspective view of the 3D bct sturucture based on the respective theoretical light intensity model. (b) The SEM image of the resultant 3D hydrogel structure with interconnected nanopore size fabricated from the phase mask shown in (a). The inset is the cross-sectional image of the structure which matches well with the inset as shown in (a).

that is caused by the passage of the incident beam through the phase mask into the photoresist results in creation of periodic structures. The light intensity distribution throughout the photoresist depends on the geometry and the refractive index of the PDMS phase mask and the refractive index of the photoresist. Figure 2a is the scanning electron microscopy (SEM) image of the phase mask. The post regions of the phase mask have a height of 350 nm and period of 760 nm. The light intensity distribution of the theoretical 3D bicontinuous structure is shown in the inset. The PMIL structure targeted here is body-centered tetragonal (bct) with $a = b = 760$ nm, c (the Talbot distance) $= 4.04$ μm which provides high porosity as well as good stability of the structure. Calculations were carried out utilizing the Fourier modal method[38] to extract polarizations and phases of the diffracted beams. Interference lithography based calculations were used for the subsequent recombination of beams and to choose the appropriate structure corresponding to a given exposure dose.[39] This PMIL nanopatterning results in the formation of connected pores at the submicrometer scale. Since the swelling of the patterned hydrogel structure in developer solution (cyclopentanone in our case) is inevitable, the resultant structure shows slight pattern collapse. However, unlike photonic or phononic applications where precise geometric periodicity is essential, modest pattern distortion does not affect the intended biological functionality. The SEM image of the resultant 3D hydrogel structure with submicrometer pore size fabricated from the phase mask in Figure 2a is shown in Figure 2b. The inset in Figure 2b is the cross-sectional image of the bicontinuous structure which matches well with the theoretical inset in Figure 2a.

To demonstrate proof of concept, we have patterned 3D hydrogels with a fully open, bicontinuous polymer/air morphology on neural prosthetic devices which can be used to deliver neurotrophins in vivo. Resist solutions were spin-coated on top of the neural prosthetic device. After exposure and development, the devices coated with a bicontinuous hydrogel/air microstructure were trimmed by a cross section polisher. An overall view of the hydrogel coatings on the device with an overall dimension of 5 mm $\times$ 123 μm $\times$ 15 μm is shown in Figure 3a at different magnifications. The high magnification image (top) clearly shows a 3D structure with open, interconnected pores. The advantage of our approach is that (a) the presence of hydrogel on the surface of the device will serve as a mechanical buffer between the tissue−device interface, (b) there will be minimum impedance change after micropattern formation, (c) neurons will more easily interface with the electrodes as compared to fully coated hydrogel devices, and (d) the hydrogel can be used to deliver neurotrophins to promote neuron growth and connection to the device and/or release anti-inflammatory drugs to reduce glial scar formation. All these combined factors can result in an efficient neuron−device interaction which could increase the useful lifetime of the device in vivo. Importantly, the material shows pH-dependent swelling properties which are of interest for controlled drug release applications. Panels b and c of Figure 3 are environmental SEM (ESEM) images of 3D hydrogels taken at 60% humidity after being soaked in pH $= 7.4$ or pH $= 4$ buffer solution for 20 min, respectively. For both pH conditions, the hydrogel increases its volume in approximately 20 min. Previously a hydrogel with high porosity exhibited similar fast response times for swelling and shrinkage.[40–42] Hydrogels under physiological conditions ($(a_s - a_o)/a_o = 57\%$ at pH $= 7.4$ where a_o is the initial in-plane lattice parameter of a tetragonal structure and a_s is the in-plane lattice parameter of the swollen structure) swelled more than hydrogels in acidic solution ($(a_s - a_o)/a_o = 15\%$ at pH $= 4$). This is because relatively higher electrostatic forces between MAA and the solute at pH $= 7.4$ induce higher swelling than that seen at pH $= 4$.

Nerve growth factor (NGF) is a neurotrophin which is essential for the survival and the growth of neuronal cells. Releasing NGF in vivo from the device could result in survival of the neurons near the device and the growth of neurons toward the device which could eventually help in improved neuron−device interaction. As a proof of principle, we have shown that NGF can be released from these networks. Figure 4 shows the release profiles of nerve growth factor from the patterned hydrogel devices. In order to exploit the pH-sensitive microstructures, the hydrogels were loaded at pH 4 and pH 7.4 and released in pH 7.4 buffer. Initially, we carried out experiments to determine the loading concentration that is required to give a total release of 50 ng of

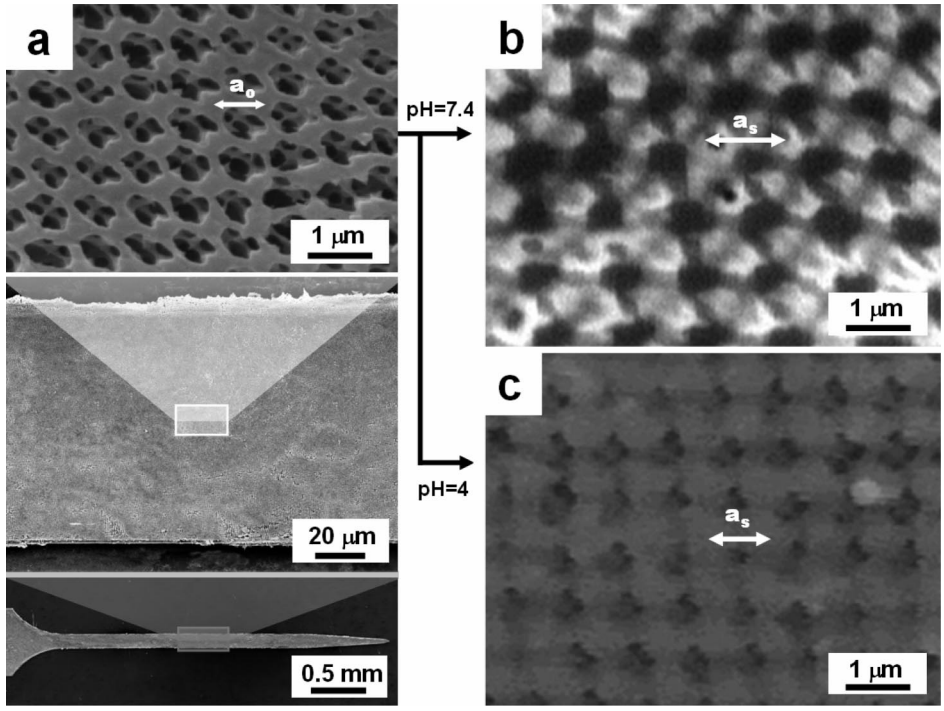

Figure 3. SEM images of 3D hydrogels coated on a neural prosthetic device. (a) View of the hydrogel coating on the device with an overall dimension of 5 mm × 123 μm × 15 μm at different magnifications. The image at the top clearly shows the 3D structure with labyrinthine air networks (a_o = initial in plane lattice parameter of tetragonal structure). (b and c) ESEM image of 3D hydrogels after being soaked in pH = 7.4 and pH = 4 buffer solution for 20 min, respectively (a_s = in plane lattice parameter of swollen structure).

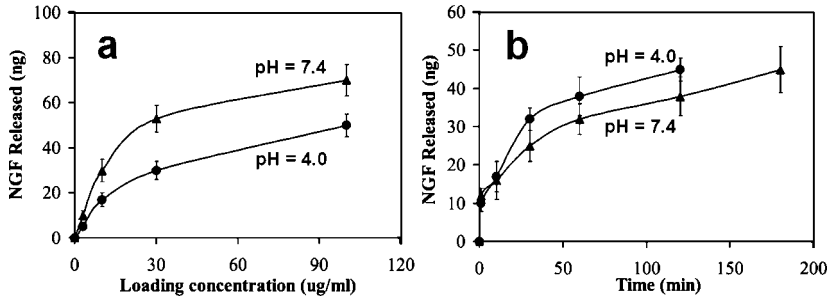

Figure 4. Release profiles of nerve growth factor from the patterned hydrogel devices under different environmental conditions. (a) Released NGF as the loading concentration of NGF is varied. (b) Release profile as a function of time when the hydrogels are loaded with 50 ng/mL NGF.

NGF in the release solution, since according to the suppliers product insert, 5−50 ng/mL is the recommended working concentration for most of the in vitro applications. The loading time was 24 h at 4–8 °C. Figure 4a shows the released NGF as the loading concentration is varied. As can be seen, when the devices are loaded at pH 7.4, the amount of NGF released is much greater than when the devices are loaded at pH 4 at the same loading concentration. This can be explained by two reasons. (1) The hydrogel swells more at pH 7.4 than at pH 4 and (2) NGF has a higher positive charge at pH 4 than at pH 7.4, since it has an isoelectric point (pI) of ~9.5, which will result in greater electrostatic repulsion between NGF and the hydrogel.

Because of these two reasons, a smaller amount of NGF will be loaded at a given concentration at pH 4.0 as compared to loading at pH 7.4. Hence a higher loading concentration will be required to incorporate the same amount of NGF at lower pH. From Figure 4a it was determined that in order to load 50 ng of NGF at pH 4, a loading concentration of 100 μg/mL is required as compared to only a 30 μg/mL at pH 7.4 to achieve the same NGF loading of the hydrogels. Figure 4b shows the release profile when the hydrogel is loaded with 50 ng/mL either at pH 4 or at pH 7.4. Both releases were done at pH 7.4. It is seen that the half-life (time taken for half of the total amount to be released) for hydrogels loaded at pH 4 is approximately 20 min compared to 30 min when the hydrogels are loaded with NGF at pH 7.4. This result occurs because the NGF that has been loaded at pH 7.4 has been more fully able to penetrate the hydrogel pores compared to the NGF loaded at pH 4.0. This pH sensitivity of the hydrogel networks can be used to develop smart drug-delivery systems. For optimal in vivo response, release times of NGF over a period of few days rather than few hours are required. However, as mentioned earlier, glial scar formation is due to both short-term and long-term responses.[7,10] The short time release of NGF can possibly counteract the short-

term responses. We are currently investigating drug-delivery systems such as encapsulation of NGF in nanaospheres to increase the release times of NGF.

In conclusion, we have synthesized a new biocompatible polymer with the ability to create fully open, bicontinuous 3D hydrogel/air networks using PMIL. We have shown that 3D patterned hydrogels could be successfully fabricated on a neural prosthetic device. We also demonstrated that the patterned hydrogel network can be employed as a smart drug-delivery system for the delivery of nerve growth factor. A 3D hydrogel/air network with nanometer scale pores will provide a simple way for neuronal connection to the device interface. The low intrinsic polymer density in the hydrogel allows for ample volume for incorporation of drugs for controlled release. Such devices give promise for novel microfabricated neural devices with enhanced performance as well as long lifetimes in vivo.

Acknowledgment. This work is supported in part by the Institute for Soldier Nanotechnologies of the U.S. Army Research Office, National Science Foundation Grant No. DMR-0414974, the Nanobiotechnology Centre (NBTC), a STC program of the National Science Foundation under Agreement Number ECS-9876771, and NIH NSR01- 044287. We thank William Shain and Matt Hynd of the New York State Wadsworth Center for helpful interactions.

Supporting Information Available: Detailed experimental procedures, NMR, and thermogravimetric analysis of the polymer. This material is available free of charge via the Internet at http://pubs.acs.org.

References

(1) Taylor, D. M.; Tillery, S. I. H.; Schwartz, A. B. *Science* **2002**, *296*, 1829.
(2) Schwartz, A. B.; Taylor, D. M.; Tillery, S. I. H. *Curr. Opin. Neurobiol.* **2001**, *11*, 701.
(3) Alesch, F.; Pinter, M. M.; Helscher, R. J.; Fertl, L.; Benabid, A. L.; Koos, W. T. *Acta Neurochir.* **1995**, *136*, 75.
(4) Hartmann, R.; Shepherd, R. K.; Heid, S.; Klinke, R. *Hear. Res.* **1997**, *112*, 115.
(5) James, C. D.; Spence, A. J. H.; Dowell-Mesfin, N. M.; Hussain, R. J.; Smith, K. L.; Craighead, H. G.; Isaacson, M. S.; Shain, W.; Turner, J. N. *IEEE Trans. Biomed. Eng.* **2004**, *51*, 1640.
(6) Drake, K. L.; Wise, K. D.; Farraye, J.; Anderson, D. J.; Bement, S. L. *IEEE Trans. Biomed. Eng.* **1988**, *35*, 719.
(7) Turner, J. N.; Shain, W.; Szarowski, D. H.; Andersen, M.; Martins, S.; Isaacson, M.; Craighead, H. *Exp. Neurol.* **1999**, *156*, 33.
(8) Schmidt, S.; Horch, K.; Normann, R. *J. Biomed. Mater. Res.* **1993**, *27*, 1393.
(9) Biran, R.; Martin, D. C.; Tresco, P. A. *Exp. Neurol.* **2005**, *195*, 115.
(10) Szarowski, D. H.; Andersen, M. D.; Retterer, S.; Spence, A. J.; Isaacson, M.; Craighead, H. G.; Turner, J. N.; Shain, W. *Brain Res.* **2003**, *983*, 23.
(11) McCreery, D. B.; Agnew, W. F.; McHardy, J. *IEEE Trans. Biomed. Eng.* **1987**, *34*, 664.
(12) Cui, X. Y.; Wiler, J.; Dzaman, M.; Altschuler, R. A.; Martin, D. C. *Biomaterials* **2003**, *24*, 777.
(13) Kim, D. H.; Abidian, M.; Martin, D. C. *J. Biomed. Mater. Res., Part A* **2004**, *71A*, 577.
(14) Wadhwa, R.; Lagenaur, C. F.; Cui, X. T. *J. Controlled Release* **2006**, *110*, 531.
(15) Khademhosseini, A.; Jon, S.; Suh, K. Y.; Tran, T. N. T.; Eng, G.; Yeh, J.; Seong, J.; Langer, R. *Adv. Mater.* **2003**, *15*, 1995.
(16) Dong, L.; Agarwal, A. K.; Beebe, D. J.; Jiang, H. R. *Nature* **2006**, *442*, 551.
(17) Kim, J.; Nayak, S.; Lyon, L. A. *J. Am. Chem. Soc.* **2005**, *127*, 9588.
(18) Kim, H.; Cohen, R. E.; Hammond, P. T.; Irvine, D. J. *Adv. Funct. Mater.* **2006**, *16*, 1313.
(19) Albrecht, D. R.; Underhill, G. H.; Wassermann, T. B.; Sah, R. L.; Bhatia, S. N. *Nat. Methods* **2006**, *3*, 369.
(20) Charles, P. T.; Goldman, E. R.; Rangasammy, J. G.; Schauer, C. L.; Chen, M. S.; Taitt, C. R. *Biosens. Bioelectron.* **2004**, *20*, 753.
(21) Luo, Y.; Shoichet, M. S. *Nat. Mater.* **2004**, *3*, 249.
(22) Moutos, F. T.; Freed, L. E.; Guilak, F. *Nat. Mater.* **2007**, *6*, 162.
(23) Tsang, V. L.; Chen, A. A.; Cho, L. M.; Jadin, K. D.; Sah, R. L.; DeLong, S.; West, J. L.; Bhatia, S. N. *FASEB J.* **2007**, *21*, 790.
(24) Zhang, Y. J.; Wang, S. P.; Eghtedari, M.; Motamedi, M.; Kotov, N. A. *Adv. Funct. Mater.* **2005**, *15*, 725.
(25) Liu, Y. F.; Wang, S. P. *Colloids Surf., B* **2007**, *58*, 8.
(26) Yeh, J.; Ling, Y. B.; Karp, J. M.; Gantz, J.; Chandawarkar, A.; Eng, G.; Blumling, J.; Langer, R.; Khademhosseini, A. *Biomaterials* **2006**, *27*, 5391.
(27) Bryant, S. J.; Cuy, J. L.; Hauch, K. D.; Ratner, B. D. *Biomaterials* **2007**, *28*, 2978.
(28) Jhaveri, S. J.; Senaratne, W.; Hynd, M. R.; Turner, J. N.; Sengupta, P.; Shain, W.; Ober, C. K. *J. Photopolym. Sci. Technol.* **2006**, *19*, 435.
(29) Jeon, S.; Park, J. U.; Cirelli, R.; Yang, S.; Heitzman, C. E.; Braun, P. V.; Kenis, P. J. A.; Rogers, J. A. *Proc. Natl. Acad. Sci. U.S.A.* **2004**, *101*, 12428.
(30) Bita, I.; Choi, T.; Walsh, M. E.; Smith, H. L.; Thomas, E. L. *Adv. Mater.* **2007**, *19*, 1403.
(31) Jang, J. H.; Dendukuri, D.; Hatton, T. A.; Thomas, E. L.; Doyle, P. S. *Angew. Chem., Int. Ed.* **2007**, *46*, 9027.
(32) Thakur, A.; Banthia, A. K.; Maiti, B. R. *J. Appl. Polym. Sci.* **1995**, *58*, 959.
(33) Rath, S. K.; Boey, F. Y. C.; Abadie, M. J. M. *Polym. Int.* **2004**, *53*, 857.
(34) Lu, S.; Anseth, K. S. *J. Controlled Release* **1999**, *57*, 291.
(35) Yang, S.; Ford, J.; Ruengruglikit, C.; Huang, Q. R.; Aizenberg, J. *J. Mater. Chem.* **2005**, *15*, 4200.
(36) Belkas, J. S.; Munro, C. A.; Shoichet, M. S.; Johnston, M.; Midha, R. *Biomaterials* **2005**, *26*, 1741.
(37) Peppas, N. A. *Int. J. Pharm.* **2004**, *277*, 11.
(38) Li, L. F. *J. Opt. Soc. Am. A* **1997**, *14*, 2758.
(39) Ullal, C. K.; Maldovan, M.; Wohlgemuth, M.; Thomas, E. L. *J. Opt. Soc. Am. A* **2003**, *20*, 948.
(40) Kabiri, K.; Zohuriaan-Mehr, M. J. *Macromol. Mater. Eng.* **2004**, *289*, 653.
(41) Vlachou, M.; Naseef, H.; Efentakis, M.; Tarantili, P. A.; Andreopoulos, A. G. *J. Biomater. Appl.* **2001**, *15*, 293.
(42) Zhao, B.; Moore, J. S. *Langmuir* **2001**, *17*, 4758.

NL080444+